Int. J. Solids Structures Vol. 22, No. 5, pp. 527–551, 1986
Printed in Great Britain.

0020–7683/86 $3.00+.00
Pergamon Journals Ltd.

HEAT CONDUCTION IN PLATES AND SHELLS WITH EMPHASIS ON A CONICAL SHELL

M. B. RUBIN
Faculty of Mechanical Engineering, Technion, Israel Institute of Technology, Haifa 32 000, Israel

(*Received* 17 *December* 1984; *in revised form* 20 *June* 1985)

Abstract—This paper is concerned with analyzing heat conduction in rigid shell-like bodies. The thermal equations of the theory of a Cosserat surface are used to calculate the average (through-the-thickness) temperature and temperature gradient directly, without resorting to integration of three-dimensional results. Specific attention is focused on a conical shell. The conical shell is particularly interesting because it has a converging geometry, so that the shell near its tip is "thick" even though the shell near its base may be "thin". Generalized constitutive equations are developed here in a consistent manner which include certain geometrical features of shells. These equations are tested by considering a number of problems of plates, circular cylindrical shells and spherical shells, and comparing the results with exact solutions. In all cases, satisfactory results are predicted even in the thick-shell limit. Finally, a problem of transient heat conduction in a conical shell is solved. It is shown that the thermal bending moment produced by the average temperature gradient is quite severe near the tip, and it attains its maximum value in a relatively short time

1. INTRODUCTION

Most aerospace structures are compositions of structural components which can be modeled as shell-like bodies. For various reasons, it is desirable to determine the thermomechanical response of these shell-like bodies to thermal and mechanical loads. Within the context of classical linear shell theory, the temperature distribution influences the mechanical response of the shell through the resultant thermal force and resultant thermal moment. For an elastic shell, the thermal force is related to the average (through-the-thickness) temperature and the thermal moment is related to the average temperature gradient by constitutive equations.

Often (when the strain rates are small and the heat flux vector is independent of strain), the thermal and mechanical problems are uncoupled in the sense that the temperature field may be determined by solving equations for a rigid heat conductor. Then the resulting temperature field may be used to calculate the thermal force and thermal moment which provide thermal loading for the determination of the deformation of the shell.

In this paper, we confine attention to the determination of the temperature distribution in a shell-like body which is treated as a rigid heat conductor. Although the temperature distribution can be determined by attempting to solve the three-dimensional heat conduction equation, this approach has two major disadvantages. First, since the thermal loads for shell theory depend only on the average temperature and temperature gradient, much of the details calculated by this approach are not of prime importance. Second, since the heat conduction equation admits separable solutions only for a limited number of geometries, it is exceedingly difficult to obtain analytical solutions for many typical shell geometries. This latter problem has been addressed in [1], where equations are developed to calculate an approximate temperature distribution in shells of revolution.

Here we take a different approach and use thermal equations for shells which have been developed[2, 3] to predict the average temperature and temperature gradient directly, without resorting to integration of three-dimensional results. The most recent of these developments[3] is based on modeling the shell-like body as a Cosserat surface. Details of this theory may be found in [3, 4]. Specifically, the objective of this paper is to determine the average temperature and temperature gradient in a conical shell (Fig. 1) which is a basic aerospace structure. The conical shell is particularly interesting because it has a converging geometry, so that the shell near its tip is necessarily "thick" even though

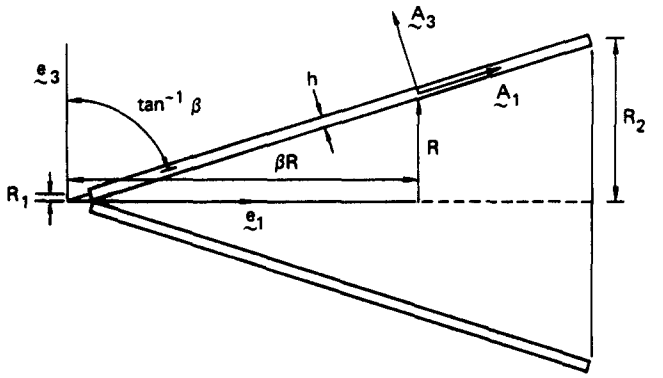

Fig. 1. Conical shell of constant thickness h, tip radius R_1 and base radius R_2.

the shell near its base may be "thin". For this reason, it is questionable whether any shell theory can accurately predict results for the critical tip region. Here it is shown that with appropriate constitutive equations, the Cosserat theory includes enough of the geometry of the shell to predict relatively accurate results for the conical shell.

It should be emphasized that it is not a trivial matter to develop equations for shells which produce reasonable results in the thick-shell limit. For example, we recall that the equations in [1] were developed by writing the heat conduction equation in a form appropriate for shells and then neglecting quantities multiplied by higher powers of the ratio of the thickness to radius of curvature. Even though these equations are more complicated than the Cosserat equations in that details of the through-the-thickness temperature distribution are calculated, too much of the shell geometry has been neglected, so that they predict inaccurate results in the thick-shell limit. The predictions of the equations in [1] are compared with the more accurate predictions of the Cosserat theory for the thick-shell problems considered in Sections 4 and 5.

In the following sections, we discuss the basic equations of the Cosserat theory and then solve a number of problems. To develop confidence in the predictions of the Cosserat theory in the base region of the conical shell, we solve various problems for a plate and compare with exact solutions in [5]. These problems examine the effect of the three types of boundary conditions on the major surfaces of the plate: specified heat flux, specified temperature and radiation. Next, to develop confidence in the predictions of the theory in the tip region of the conical shell, we use the same equations to solve specific problems for a solid circular cylinder and a solid sphere, and compare the results with exact solutions. Finally, after having developed confidence in the predictions of the theory in both the tip and base regions of the conical shell, we solve a specific heat conduction problem for a conical shell.

2. BASIC EQUATIONS

Let the material points of the Cosserat surface C be identified by means of a system of convected coordinates θ^α ($\alpha = 1, 2$) and let the two-dimensional region of space occupied by the material surface in the present configuration at time t be denoted by c. Further, let the vector-valued function $\mathbf{r}$ define the position of a material point of the surface C and at each such point define the vector valued function $\mathbf{d}$, called the director, and the two temperature fields θ and ϕ, each referred to the present configuration. Then a thermomechanical process of the Cosserat surface is defined by

$$\mathbf{r} = \mathbf{r}(\theta^\alpha, t), \qquad \mathbf{d} = \mathbf{d}(\theta^\alpha, t), \qquad [\mathbf{a}_1\mathbf{a}_2\mathbf{d}] > 0, \tag{2.1a, b, c}$$

$$\theta = \theta(\theta^\alpha, t), \qquad (\theta > 0), \qquad \phi = \phi(\theta^\alpha, t), \tag{2.1d, e, f}$$

where the tangent vectors $\mathbf{a}_\alpha$ and the unit normal vector $\mathbf{a}_3$ are defined by

$$\mathbf{a}_\alpha = \frac{\partial \mathbf{r}}{\partial \theta^\alpha}, \quad \mathbf{a}_\alpha \cdot \mathbf{a}_3 = 0, \quad \mathbf{a}_3 \cdot \mathbf{a}_3 = 1, \quad a^{1/2} = [\mathbf{a}_1 \mathbf{a}_2 \mathbf{a}_3] > 0, \qquad (2.2a, b, c, d)$$

and the condition (2.1c) ensures that the director is nowhere tangent to c. Also, in the above, θ represents the average (through-the-thickness) temperature in the shell, and ϕ represents the average temperature gradient.

In the reference configuration, we assume that the shell has uniform thickness h and is at uniform temperature θ_0. Then the reference values of the various kinematic quantities may be denoted by†

$$\mathbf{r} = \mathbf{R}, \qquad \mathbf{d} = \mathbf{D} = \mathbf{A}_3, \qquad \mathbf{a}_i = \mathbf{A}_i, \qquad a^{1/2} = A^{1/2}, \qquad (2.3a, b, c, d)$$

$$\theta = \theta_0, \qquad \phi = 0, \qquad (2.3e, f)$$

where $\mathbf{R}$, $\mathbf{A}_i$ and $A^{1/2}$ depend on the coordinates θ^α only. For the rigid heat conductor considered here, there is no distinction between the reference and the present configurations, so that eqns (2.3a–d) hold for all time. Further, all tensor quantities will be referred to the base vectors $\mathbf{A}_i$ and their reciprocals $\mathbf{A}^i$ defined by

$$\mathbf{A}_i \cdot \mathbf{A}^j = \delta_i^j, \qquad (2.4)$$

where δ_i^j is the Kronecker symbol.

Let P, bounded by the closed curve ∂P, denote the region occupied by an arbitrary material portion of the surface c, and let ν be the unit outward normal to ∂P. Using the notation of [3], we define the following quantities: the positive mass density (mass per unit area of P) in the reference configuration $\rho_0 = \rho_0(\theta^\alpha)$; the specific (per unit mass of P) entropies $\eta = \eta(\theta^\alpha, t)$ and $\eta_1 = \eta_1(\theta^\alpha, t)$; the specific internal rates of production of entropy $\xi = \xi(\theta^\alpha, t)$, $\xi_1 = \xi_1(\theta^\alpha, t)$ and $\bar{\xi}_1 = \bar{\xi}_1(\theta^\alpha, t)$; the entropy fluxes $k = k(\theta^\alpha, t; \nu)$ and $k_1 = (\theta^\alpha, t; \nu)$, each per unit length of the curve ∂P; the specific external rates of supply of entropy $s = s(\theta^\alpha, t)$ and $s_1 = (\theta^\alpha, t)$; the specific internal energy $\varepsilon = \varepsilon(\theta^\alpha, t)$; and the specific Helmholtz free energy $\psi = \psi(\theta^\alpha, t) \equiv \varepsilon - \theta\eta - \phi\eta_1$. With suitable continuity assumptions, it can be shown that[3, 4]

$$k = \mathbf{p} \cdot \nu = p^\alpha \nu_\alpha, \qquad k_1 = \mathbf{p}_1 \cdot \nu = p_1^\alpha \nu_\alpha, \qquad (2.5a, b)$$

where $\nu_\alpha = \mathbf{A}_\alpha \cdot \nu$ are the components of the normal vector ν and where we use the usual summation convention over repeated indices. Further, with reference to the energy equation, the specific external rates of heat supply r and r_1; and the heat flux vectors $\mathbf{q}$ and $\mathbf{q}_1$ are defined by

$$r = \theta s, \qquad r_1 = \phi s_1, \qquad \mathbf{q} = \theta \mathbf{p}, \qquad \mathbf{q}_1 = \phi \mathbf{p}. \qquad (2.6a, b, c, d)$$

Now the local forms of the balances of entropy may be recorded as[3]

$$\rho_0 \dot{\eta} = \rho_0(s + \xi) - p^\alpha|_\alpha, \qquad \rho_0 \dot{\eta}_1 = \rho_0(s_1 + \xi_1) - p_1^\alpha|_\alpha, \qquad (2.7a, b)$$

where a dot denotes material time differentiation and where a bar denotes covariant differentiation with respect to the metric $A_{\alpha\beta}$ of the shell surface. For later convenience, we recall[3, 4] definitions for the metric tensor $A_{\alpha\beta}$, and its reciprocal $A^{\alpha\beta}$, the curvature tensor $B_{\alpha\beta}$, the Christoffel symbol $\Gamma_{\alpha\beta}^\sigma$, and covariant differentiation in the forms

$$A_{\alpha\beta} = \mathbf{A}_\alpha \cdot \mathbf{A}_\beta, \qquad A^{\alpha\beta} = \mathbf{A}^\alpha \cdot \mathbf{A}^\beta, \qquad B_{\alpha\beta} = A_{\alpha,\beta} \cdot \mathbf{A}_3, \qquad (2.8a, b, c)$$

† Throughout the text, Greek indices have a range (1, 2) and Latin indices have a range (1, 2, 3).

$$\Gamma^{\sigma}_{\alpha\beta} = \mathbf{A}_{\alpha,\beta}\cdot\mathbf{A}^{\sigma}, \qquad \theta|_{\alpha} = \theta_{,\alpha}, \qquad p^{\sigma}|_{\beta} = p^{\sigma}_{,\beta} + \Gamma^{\sigma}_{\alpha\beta}p^{\alpha}, \tag{2.8d, e, f}$$

where a comma denotes partial differentiation with respect to θ^{α}.

Equations (2.7) must be supplemented by an energy equation and constitutive equations. It follows from [3] that the energy equation for a rigid thermoelastic shell is satisfied provided that

$$\eta = -\partial\psi/\partial\theta, \qquad \eta_1 = -\partial\psi/\partial\phi \tag{2.9a, b}$$

and

$$\rho_0\theta\xi + \rho_0\phi\xi_1 + \mathbf{p}\cdot\mathbf{g} + \mathbf{p}_1\cdot\mathbf{g}_1 = 0, \tag{2.10}$$

where the temperature gradients $\mathbf{g}$ and $\mathbf{g}_1$ are defined by

$$\mathbf{g} = \theta_{,\alpha}\mathbf{A}^{\alpha}, \qquad \mathbf{g}_1 = \phi_{,\alpha}\mathbf{A}^{\alpha}. \tag{2.11a, b}$$

Confining attention to a rigid shell which is thermally isotropic, we specify constitutive equations in the form

$$2\rho_0\psi = -\beta_3(\theta^2 - 2\theta\theta_0) - \beta_4\phi^2 - 2\beta_5\theta, \tag{2.12a}$$

$$\mathbf{p} = -a_0\mathbf{g}, \qquad \mathbf{p}_1 = -b_1\mathbf{g}_1, \tag{2.12b, c}$$

$$\rho_0\theta\xi = a_0\mathbf{g}\cdot\mathbf{g} + b_1\mathbf{g}_1\cdot\mathbf{g}_1 + b_2\phi^2, \tag{2.12d}$$

$$\rho_0\xi_1 = \rho_0\xi^1 = -b_2\phi, \tag{2.12e}$$

where $a_0, b_1, b_2, \beta_3 - \beta_5$ are constants. Substituting (2.12a) into (2.9) we have

$$\rho_0\eta = \beta_3(\theta - \theta_0) + \beta_5, \qquad \rho_0\eta_1 = \beta_4\phi. \tag{2.13a, b}$$

The form of the constitutive equations (2.12) represents a slight generalization of those introduced in [3] for the linear theory.† These equations are chosen to automatically satisfy the reduced energy eqn (2.10) without approximation.

In postulating the form of the constitutive equations (2.12), there is a tacit assumption that constitutive equations which are valid for a plate are also valid for a shell. In the discussion in Section 5, we observe that certain geometrical features of the shell must be included in the constitutive equations to predict relatively accurate results for a solid sphere. These geometrical features of the shell may be introduced by appropriately modifying the constitutive equations to take the forms

$$2\rho_0^*h\psi = -\beta_3(\theta^2 - 2\theta\theta_0) - \beta_4\phi^2 - 2\beta_5\theta, \tag{2.14a}$$

$$\mathbf{p} = -a_0\mathbf{g}, \qquad \mathbf{p}_1 = -b_1\mathbf{g}_1, \tag{2.14b, c}$$

$$\rho_0\theta\xi = a_0\mathbf{g}\cdot\mathbf{g} + b_1\mathbf{g}_1\cdot\mathbf{g}_1 + (\rho_0/\rho_0^*h)b_2\phi^2, \tag{2.14d}$$

$$\rho_0^*h\xi_1 = \rho_0^*h\xi^1 = -b_2\phi, \tag{2.14e}$$

$$\rho_0\eta = (\rho_0/\rho_0^*h)[\beta_3(\theta - \theta_0) + \beta_5], \qquad \rho_0\eta_1 = (\rho_0/\rho_0^*h)\beta_4\phi, \tag{2.14f, g}$$

† The sign convention associated with the constants β_3, β_4 used here is chosen to be opposite from that used in [3] to make β_3 and β_4 positive quantities.

where ρ_0^* is the constant three-dimensional mass density (mass per unit volume) of the material, and h is the constant thickness of the shell. The constitutive equations (2.14f, g) depend on the geometry of the shell through the ratio $\rho_0/\rho_0^* h$ [see eqn (2.17a)].

Within the context of the general theory, the constitutive equations must be further restricted by statements of the second law of thermodynamics[3]. For either of the sets of constitutive equations (2.12) and (2.13) or (2.14), these restrictions reduce to

$$a_0 \geqslant 0, \qquad b_1 \geqslant 0, \qquad b_2 \geqslant 0, \qquad \beta_3 > 0. \tag{2.15a, b, c, d}$$

To linearize the equations presented above, we assume that the temperatures $(\theta - \theta_0)$ and ϕ, and their space and time derivatives are small enough that quadratic expressions in these quantities may be neglected relative to linear expressions. It follows from (2.12d) or (2.14d) that ξ is of higher order so that ξ may be set equal to zero in (2.7a).

Now we recall[3, 4] that the Cosserat theory which is developed by direct approach may be brought into a one-to-one correspondence with the three-dimensional theory by assuming that the position vector $\mathbf{r}^*$ of a point in the shell and the temperature field θ^* admit the representations

$$\mathbf{r}^* = \mathbf{r}^*(\theta^\alpha, \theta^3, t) = \mathbf{r}(\theta^\alpha, t) + \theta^3 \mathbf{d}(\theta^\alpha, t), \tag{2.16a}$$

$$\theta^* = \theta^*(\theta^\alpha, \theta^3, t) = \theta(\theta^\alpha, t) + \theta^3 \phi(\theta^\alpha, t), \tag{2.16b}$$

where θ^3 is a coordinate through the thickness of the shell. For a shell of constant thickness h, we may choose the reference surface of the shell to be the middle surface and define the top surface ∂P^+ of the shell by $\theta^3 = h/2$ and the bottom surface ∂P^- by $\theta^3 = -h/2$. If the three-dimensional mass density ρ_0^* of the shell is constant, then it may be shown that[3, 4, 6]

$$\lambda = \rho_0 A^{1/2} = \int_{-h/2}^{h/2} \rho_0^* G^{1/2} \, \mathrm{d}\theta^3 = (\rho_0^* h A^{1/2})[1 + (h^2/12)(B_1^1 B_2^2 - B_1^2 B_2^1)], \tag{2.17a}$$

$$\lambda s = \lambda \hat{s} - B^+ k^+ - B^- k^-, \qquad \lambda \hat{s} = \int_{-h/2}^{h/2} \rho_0^* s^* G^{1/2} \, \mathrm{d}\theta^3, \tag{2.17b, c}$$

$$\lambda s_1 = \lambda \hat{s}_1 - (h/2) B^+ k^+ + (h/2) B^- k^-, \qquad \lambda \hat{s}_1 = \int_{-h/2}^{h/2} \rho_0^* s^* G^{1/2} \theta^3 \, \mathrm{d}\theta^3, \tag{2.17d, e}$$

$$G^{1/2} = A^{1/2}[1 - \theta^3 B_\sigma^\sigma + (\theta^3)^2 (B_1^1 B_2^2 - B_1^2 B_2^1)], \tag{2.17f}$$

$$B^+ = A^{1/2}[1 - (h/2) B_\sigma^\sigma + (h^2/4)(B_1^1 B_2^2 - B_1^2 B_2^1)], \tag{2.17g}$$

$$B^- = A^{1/2}[1 + (h/2) B_\sigma^\sigma + (h^2/4)(B_1^1 B_2^2 - B_1^2 B_2^1)], \tag{2.17h}$$

$$\theta^+ = \theta + (h/2)\phi, \qquad \theta^- = \theta - (h/2)\phi, \tag{2.17i, j}$$

where s^* is the three-dimensional rate of entropy supply; k^+ and k^- are, respectively, the entropy fluxes applied to the major surfaces ∂P^+ and ∂P^-; B_β^α are the mixed components of the curvature tensor; and θ^+ and θ^- are, respectively, the temperatures on the major surfaces ∂P^+ and ∂P^-. Also, we note that for the linear theory,

$$\theta_0 k^+ = q^+, \qquad \theta_0 k^- = -q^-, \tag{2.18a, b}$$

where q^+ is the heat flux measured positive for heat flowing out of the surface ∂P^+, and q^- is the heat flux measured positive for heat flowing into the surface ∂P^-.

Most of the constitutive coefficients were evaluated in [3] by direct integration of the three-dimensional constitutive equations. An alternative approach was taken in [6], where the coefficients were evaluated by comparing Cosserat solutions with exact three-dimensional solutions. Except for the value of β_3, the results in [3] and [6] are the same. Here we adopt the results in [6] and specify

$$a_0 = Kh/\theta_0, \qquad b_1 = Kh^3/12\theta_0, \qquad b_2 = Kh/\theta_0, \tag{2.19a, b, c}$$

$$\beta_3 = \rho_0^* ch/\theta_0, \qquad \beta_4 = \rho_0^* ch^3/\pi^2\theta_0, \tag{2.19d, e}$$

where K is the thermal conductivity, and c is the specific heat at constant strain of the material. The coefficient β_5 corresponds to the arbitrary constant reference value of the entropy and therefore cannot be specified. Since the material constants K and c are positive, we realize from (2.19) that the restrictions (2.15) are satisfied.

Finally, we use (2.14) and (2.17)–(2.19) to write the linearized version of eqns (2.7) in the form

$$\rho_0 c\dot{\theta} = \rho_0\theta_0\hat{s} - A^{-1/2}[B^+q^+ - B^-q^-] + Kh\nabla^2\theta, \tag{2.20a}$$

$$(\rho_0 ch^2/\pi^2)\dot{\phi} = \rho_0\theta_0\hat{s}_1 - A^{-1/2}(h/2)[B^+q^+ + B^-q^-] - (\rho_0/\rho_0^* h)Kh\phi + (Kh^3/12)\nabla^2\phi, \tag{2.20b}$$

where the Laplacian operator ∇^2 is defined by

$$\nabla^2\theta = A^{\alpha\beta}\theta|_{\alpha\beta} = A^{\alpha\beta}(\theta_{,\alpha\beta} - \Gamma^{\sigma}_{\alpha\beta}\theta_{,\sigma}). \tag{2.21}$$

3. PLATES

In this section, we examine the validity of the Cosserat theory in the thin-shell limit by considering three problems of heat conduction in a plate. These problems are chosen to examine the effects of specifying heat flux, temperature or radiation-type boundary conditions on the major surfaces of the plate. For each of these problems, we neglect external entropy supply (or external heat supply) and consider temperature fields which are functions of time, only so that

$$\hat{s} = 0, \qquad \hat{s}_1 = 0, \qquad \theta = \theta(t), \qquad \phi = \phi(t). \tag{3.1a, b, c, d}$$

Further, the curvature tensor $B_{\alpha\beta}$ for a plate vanishes. Hence from (2.17) we deduce that

$$B_{\alpha\beta} = 0, \qquad \rho_0 = \rho_0^* h, \qquad B^+ = A^{1/2}, \qquad B^- = A^{1/2}, \tag{3.2a, b, c, d}$$

and that eqns (2.20) reduce to

$$\rho_0^* ch\dot{\theta} = -q^+ + q^-, \tag{3.3a}$$

$$(\rho_0^* ch^2/\pi^2)\dot{\phi} = -\tfrac{1}{2}q^+ - \tfrac{1}{2}q^- - K\phi. \tag{3.3b}$$

Problem 1: For this problem, the heat flux q^+ is specified to be constant on the top surface, the bottom surface is insulated, and the plate is initially at uniform temperature θ_0. Mathematically, these conditions are characterized by

$$q^+ = \text{const}, \qquad q^- = 0, \tag{3.4a, b}$$

$$\theta = \theta_0, \qquad \phi = 0, \qquad \text{at } t = 0. \tag{3.4c, d}$$

Since the solution of eqns (3.3) with the conditions (3.4) was developed in [6], we merely record the solution in the nondimensional form

$$-K(\theta-\theta_0)/hq^+ = \tau, \qquad -K\phi/q^+ = \tfrac{1}{2}[1-\exp(-\pi^2\tau)], \tag{3.5a, b}$$

where τ is the nondimensional time parameter defined by

$$\tau = Kt/\rho_0^* ch^2. \tag{3.6}$$

Recall from [6] that the constitutive coefficients were chosen by requiring the Cosserat solution to compare very well with the exact solution recorded in [5] (p. 112).

To exhibit this comparison graphically, we have used (2.16b) to plot in Fig. 2 the Cosserat solution (3.5) together with the exact solution for various values of the time parameter τ. The dashed lines in Fig. 2 have been taken directly from [5] (Fig. 15, p. 113) and

$$x = \theta^3 + h/2, \tag{3.7}$$

so that $x = 0$ locates the bottom surface ∂P^-, and $x = h$ locates the top surface ∂P^+.

Problem 2: For this problem, the temperature θ^+ is specified as θ_0 on the top surface, the heat flux q^- is specified to be constant on the bottom surface, and the plate is initially at uniform temperature θ_0. Mathematically, these conditions are characterized by

$$\theta^+ = \theta_0, \qquad q^- = \text{const}, \tag{3.8a, b}$$

$$\theta = \theta_0, \qquad \phi = 0, \qquad \text{at } t = 0. \tag{3.8c, d}$$

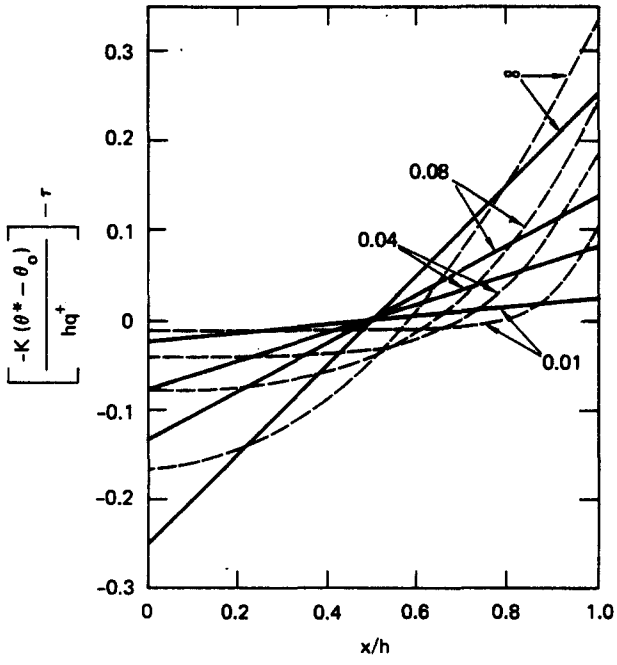

Fig. 2. Normalized temperature in a plate of thickness h, with zero heat flux at $x = 0$, constant heat flux q^+ (out of the plate) at $x = h$ and uniform initial temperature $\theta = \theta_0$. The numbers on the curves are values of $\tau = Kt/\rho_0^* ch^2$. The dashed lines are the exact solution, and the solid lines are the Cosserat solution.

With the help of (2.17i), condition (3.8a) yields

$$\theta = \theta_0 - (h/2)\phi. \tag{3.9}$$

It is important to observe here that by specifying θ^+, we tacitly specify θ in terms of ϕ through eqn (2.17i). It follows that it is not possible to specify independent initial values for θ and ϕ such as (3.8c, d). In other words, when temperature is specified on one or both of the major surfaces, we must, in general, modify the initial conditions. However, in the special case of this problem, conditions (3.8c, d) are consistent with (3.9).

Since θ^+ is specified, the heat flux q^+ must be determined from eqns (3.3). Thus, using (3.9) in (3.3a), we deduce that

$$q^+ = q^- + (\rho_0^* ch^2/2)\dot{\phi}. \tag{3.10}$$

Substituting (3.10) into (3.3b), we have

$$\rho_0^* ch^2\left(\frac{4+\pi^2}{4\pi^2}\right)\dot{\phi} + K\phi = -q^-. \tag{3.11}$$

Now solving (3.11) subject to the initial condition (3.8d), we may write the normalized solution in the form

$$\frac{K(\theta-\theta_0)}{hq^-} = \frac{1}{2}\left[1-\exp\left\{-\left(\frac{4\pi^2}{4+\pi^2}\right)\tau\right\}\right], \tag{3.12a}$$

$$\frac{-K\phi}{q^-} = \left[1-\exp\left\{-\left(\frac{4\pi^2}{4+\pi^2}\right)\tau\right\}\right], \tag{3.12b}$$

$$\frac{q^+}{q^-} = \left[1-\left(\frac{2\pi^2}{4+\pi^2}\right)\exp\left\{-\left(\frac{4\pi^2}{4+\pi^2}\right)\tau\right\}\right], \tag{3.12c}$$

where τ is defined by (3.6).

To compare the Cosserat solution (3.12) with the exact solution recorded in [5] (p. 113), we rewrite the exact solution in the form

$$\frac{K(\theta^*-\theta_0)}{hq^-} = (1/2-\theta^3) - \frac{8}{\pi^2}\sum_{n=0}^{\infty}\frac{(-1)^n}{(2n+1)^2}\sin\left[\left(\frac{2n+1}{2}\right)\pi(1/2-\theta^3)\right]\exp\left[-\frac{(2n+1)^2\pi^2}{4}\tau\right]. \tag{3.13}$$

Let us define the average temperature θ^*_{avg} and average temperature gradient ϕ^*_{avg} in the plate by the equations

$$\theta^*_{avg} - \theta_0 = \frac{1}{h}\int_{-h/2}^{h/2}(\theta^*-\theta_0)\,d\theta^3, \tag{3.14a}$$

$$\phi^*_{avg} = \frac{12}{h^3}\int_{-h/2}^{h/2}(\theta^*-\theta_0)\theta^3\,d\theta^3. \tag{3.14b}$$

Then substituting (3.13) into (3.14) and performing the integration, we deduce the results

$$\frac{K(\theta^*_{avg}-\theta_0)}{hq^-} = \frac{1}{2}\left[1-\frac{32}{\pi^3}\sum_{n=0}^{\infty}\frac{(-1)^n}{(2n+1)^3}\exp\left\{-\frac{(2n+1)^2\pi^2}{4}\tau\right\}\right], \tag{3.15a}$$

$$\frac{-K\phi^*_{avg}}{q^-} = 1 - \frac{96}{\pi^4}\sum_{n=0}^{\infty}\left[\frac{4-(2n+1)\pi(-1)^n}{(2n+1)^4}\right]\exp\left[-\frac{(2n+1)^2\pi^2}{4}\tau\right]. \qquad (3.15b)$$

Since the quantities θ and ϕ in the Cosserat solution correspond to θ^*_{avg} and ϕ^*_{avg}, we have plotted each of these in Fig. 3. The solid lines correspond to normalized values of θ and ϕ, and the dashed lines correspond to normalized values of θ^*_{avg} and ϕ^*_{avg}. The comparison for all values of τ seems quite acceptable.

Problem 3: For this problem, we consider a plate of thickness $2h$. The heat flux is specified appropriately for radiation from both the top and bottom surfaces, and the plate is initially at a uniform temperature $\theta_0 + V$. Mathematically, these conditions are characterized by

$$q^+ = KH(\theta^+ - \theta_0), \qquad q^- = -KH(\theta^- - \theta_0), \qquad (3.16a,b)$$

$$\theta = \theta_0 + V, \qquad \phi = 0, \qquad \text{at} \quad t = 0, \qquad (3.16c,d)$$

where H is a constant specifying thermal radiation from the major surfaces. First, we will solve the problem as it is formulated in (3.16), and second we will obtain a more accurate solution by exploiting the symmetry about the center plane.

For the first solution, we substitute (2.17i,j) and (3.16a,b) into eqns (3.3) and then replace h by $2h$ to obtain

$$\rho^*_0 ch\dot{\theta} = -KH(\theta - \theta_0), \qquad (4\rho^*_0 ch^2/\pi^2)\dot{\phi} = -K(1+Hh)\phi. \qquad (3.17a,b)$$

Using the initial conditions (3.16c,d), the solution of (3.17) becomes

$$(\theta - \theta_0)/V = \exp(-Hh\tau), \qquad \phi = 0, \qquad (3.18a,b)$$

where τ is again defined by (3.6). To compare the Cosserat solution (3.18) with the exact

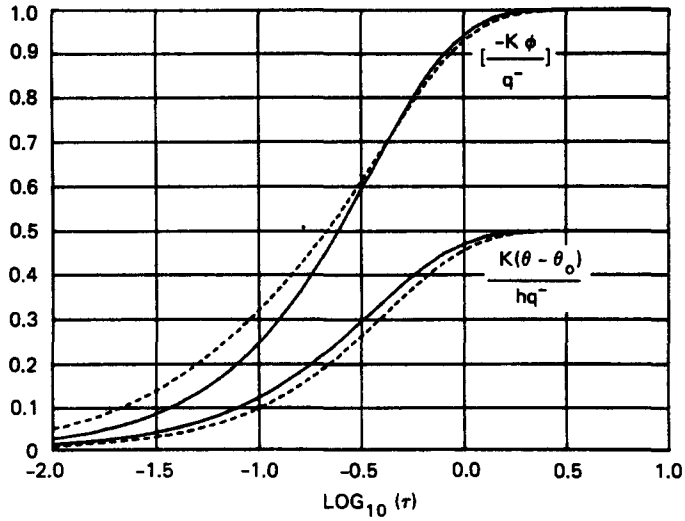

Fig. 3. Values of the normalized average temperature $[K(\theta+\theta_0)/hq^-]$ and average temperature gradient $[-K\phi q^-]$ for a plate of thickness h with heat flux q^- (entering the plate) at its bottom surface and the temperature $\theta^+ = \theta_0$ specified on the top surface. Initially, the temperature $\theta^- = \theta_0$ at the bottom surface. The dashed lines are the exact solution, and the solid lines are the Cosserat solution. $\tau = Kt/\rho^*_0 ch^2$.

solution recorded in [5] (p. 122), we rewrite the exact solution in the form

$$\frac{\theta^*-\theta_0}{V}=\sum_{n=1}^{\infty}\frac{2Hh\cos(\alpha_n\theta^3/h)\sec\alpha_n}{[(Hh)^2+Hh+\alpha_n^2]}\exp(-\alpha_n^2\tau), \tag{3.19a}$$

$$\alpha_n\tan\alpha_n=Hh, \tag{3.19b}$$

where α_n are the positive roots of equation (3.19b) and where $\theta^3=0$ locates the center of the plate, $\theta^3=h$ locates the top surface, and $\theta^3=-h$ locates the bottom surface. Replacing h by $2h$ in (3.14) and using (3.19), we deduce the expressions

$$\frac{\theta^*_{avg}-\theta_0}{V}=\sum_{n=1}^{\infty}\frac{2(Hh)^2}{\alpha_n^2[(Hh)^2+Hh+\alpha_n^2]}\exp(-\alpha_n^2\tau), \tag{3.20a}$$

$$\phi^*_{avg}=0. \tag{3.20b}$$

Comparing (3.18b) with (3.20b), we see that the Cosserat theory predicts the correct value for the average temperature gradient. To compare the prediction of the average temperature, we have plotted (3.18a) as the solid lines and (3.20a) as the dashed lines in Fig. 4 for three values of the normalized radiation coefficient Hh. From Fig. 4, we observe that for small values of Hh, the Cosserat theory predicts accurate results, whereas for large values of Hh, it does not. This is because for small values of Hh, heat is radiated slowly away from the major surfaces of the plate, so that the temperature through the thickness of the plate is nearly uniform, as predicted by (3.18b). However, for large values of Hh, heat is radiated rapidly away from the plate, and the through-the-thickness temperature gradient may be steep.

Mathematically, we may exploit the symmetry in the problem stated above and thus confine attention only to the upper half of the plate. Therefore, for this second solution, we consider a plate of thickness h. The heat flux is specified appropriately for radiation from the top surface; the bottom surface (which corresponds to the center surface of the plate of thickness $2h$) is insulated, and the plate is initially at a uniform temperature θ_0+V.

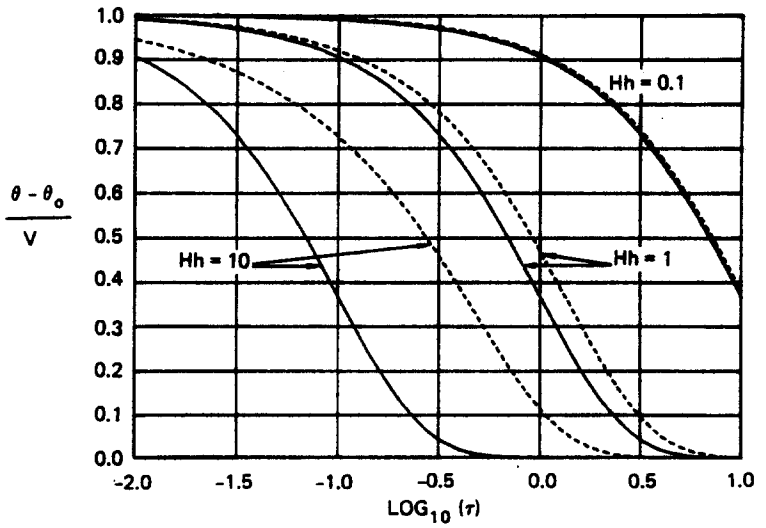

Fig. 4. Values of the normalized average temperature $(\theta-\theta_0)/V$ for a plate of thickness $2h$ with radiation from its surfaces [i.e. $q^+=KH(\theta^+-\theta_0)$] and uniform initial temperature $\theta=\theta_0+V$. The dashed lines are the exact solution, and the solid lines are the Cosserat solution. $\tau=Kt/\rho^*_0ch^2$.

These conditions are characterized by (3.16) with (3.16b) replaced by

$$q^- = 0. \tag{3.21}$$

At this point, it is important to note that although the exact solutions of the two problems considered here are identical, the Cosserat solution of the second problem will be more accurate than the Cosserat solution of the first problem. This is because the solution of the second problem admits a nonzero temperature gradient in the top half of the plate.

Substituting (2.17i), (3.16a) and (3.21) into eqns (3.3), we obtain

$$\rho_0^* ch\dot{\theta} = -KH[\theta+(h/2)\phi-\theta_0], \tag{3.22a}$$

$$\frac{\rho_0^* ch^2}{\pi^2}\dot{\phi} = -\tfrac{1}{2}KH[\theta+(h/2)\phi-\theta_0]-K\phi. \tag{3.22b}$$

In their present form, these equations are coupled. However, by solving (3.22a) for ϕ and substituting the result into (3.22b), we may define

$$(\theta-\theta_0)/V = f(\tau), \tag{3.23}$$

and write

$$-\frac{h\phi}{V} = 2f(\tau)+\frac{2}{Hh}\frac{df}{d\tau}, \qquad \frac{d^2f}{d\tau^2}+B\frac{df}{d\tau}+Cf = 0, \tag{3.24a, b}$$

where B and C are constants defined by

$$B = \pi^2+Hh+(\pi^2/4)Hh, \qquad C = \pi^2 Hh, \tag{3.25a, b}$$

and τ is defined by (3.6). Using (3.6), (3.23) and (3.24a), the initial conditions (3.16c, d) become

$$f = 1, \qquad df/d\tau = -Hh, \qquad \text{at } \tau = 0. \tag{3.26a, b}$$

Solving (3.24b) subject to the conditions (3.26), the Cosserat solution may be written in the form

$$(\theta-\theta_0)/V = A_1\exp(-\sigma_1\tau)+A_2\exp(-\sigma_2\tau), \tag{3.27a}$$

$$-\frac{h\phi}{V} = 2[A_1\exp(-\sigma_1\tau)+A_2\exp(-\sigma_2\tau)] -(2/Hh)[A_1\sigma_1\exp(-\sigma_1\tau)+A_2\sigma_2\exp(-\sigma_2\tau)], \tag{3.27b}$$

where the constants $A_1, A_2, \sigma_1, \sigma_2$ are given by

$$A_1 = \frac{\sigma_2-Hh}{\sigma_2-\sigma_1}, \qquad A_2 = \frac{Hh-\sigma_1}{\sigma_2-\sigma_1}, \tag{3.28a, b}$$

$$\sigma_1 = \tfrac{1}{2}[B-(B^2-4C)^{1/2}], \qquad \sigma_2 = \tfrac{1}{2}[B+(B^2-4C)^{1/2}]. \tag{3.28c, d}$$

Replacing θ^3 in (3.19a) by $h/2+\theta^3$, we may write the exact solution for the top half of the plate as

$$\frac{\theta^*-\theta_0}{V} = \sum_{n=1}^{\infty}\frac{2Hh\cos\{\alpha_n(h+2\theta^3)/2h\}\sec\alpha_n}{[(Hh)^2+Hh+\alpha_n^2]}\exp(-\alpha_n^2\tau), \tag{3.29}$$

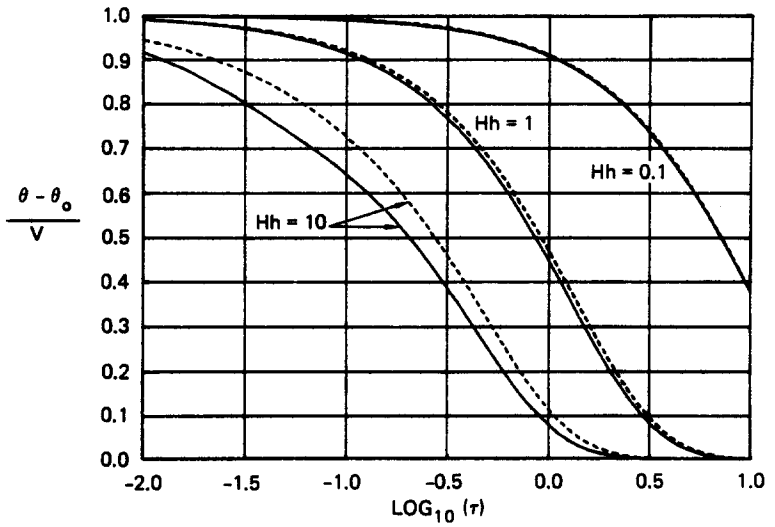

Fig. 5. Values of the normalized average temperature $(\theta-\theta_0)/V$ for a plate of thickness h with radiation from its top surface [i.e. $q^+ = KH(\theta^+-\theta_0)$], zero heat flux on its bottom surface, and uniform initial temperature $\theta = \theta_0+V$. The dashed lines are the exact solution, and the solid lines are the Cosserat solution. $\tau = Kt/\rho_0^* ch^2$.

where α_n are the positive roots of (3.19b), and where $\theta^3 = h/2$ locates the top surface, and $\theta^3 = -h/2$ locates the bottom surface (which corresponds to the center surface of the plate of thickness $2h$). Substituting (3.29) into the definitions (3.14a, b), we obtain the result (3.20a) for the average temperature θ^*_{avg} and the result

$$-\frac{h\phi^*_{avg}}{V} = -12\sum_{n=1}^{\infty}\frac{Hh[\alpha_n\sin\alpha_n+2(\cos\alpha_n-1)]\sec\alpha_n}{\alpha_n^2[(Hh)^2+Hh+\alpha_n^2]}\exp(-\alpha_n^2\tau). \tag{3.30}$$

Figure 5 compares values of the average temperature with (3.27a) plotted as the solid lines and (3.20a) plotted as the dashed lines. Similarly, Fig. 6 compares values of the average

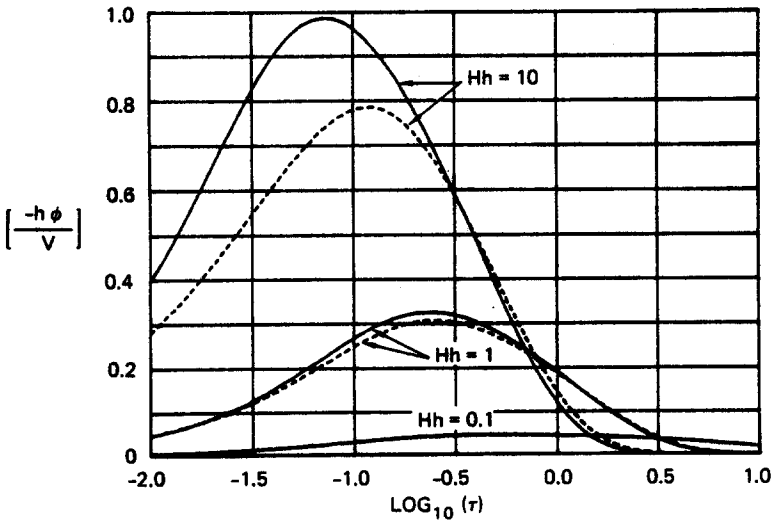

Fig. 6. Values of the normalized average temperature gradient $[-h\phi/V]$ for a plate of thickness h with radiation from its top surface [i.e. $q^+ = KH(\theta^+-\theta_0)$], zero heat flux on its bottom surface, and uniform initial temperature $\theta = \theta_0+V$. The dashed lines are the exact solution, and the solid lines are the Cosserat solution. $\tau = Kt/\rho_0^* ch^2$.

temperature gradient with (3.27b) plotted as the solid lines and (3.30) plotted as the dashed lines. From Figs. 4 and 5, we observe that modeling only the upper half of the plate produces a significant improvement in the prediction of the average temperature for the higher values of Hh. Also, we observe from Figs. 5 and 6 that, for $Hh = 0.1$, the Cosserat and exact solutions are nearly identical, and the average temperature gradient remains relatively small.

4. CIRCULAR CYLINDRICAL SHELLS

In this section, we investigate the validity of the Cosserat theory in the thick-shell limit by considering heat conduction in a circular cylindrical shell and taking the limit of a solid cylinder. Specifically, consider a circular cylindrical shell of uniform thickness h and mean radius R. Let $\mathbf{e}_i$ $(i = 1, 2, 3)$ be a set of fixed Cartesian base vectors, and let $\mathbf{e}'_i$ be base vectors of a polar coordinate system with polar angle γ defined by†

$$\mathbf{e}'_1 = \mathbf{e}_1, \qquad \mathbf{e}'_2 = \cos\gamma\mathbf{e}_2 - \sin\gamma\mathbf{e}_3, \qquad \mathbf{e}'_3 = \sin\gamma\mathbf{e}_2 + \cos\gamma\mathbf{e}_3, \qquad (4.1a, b, c)$$

where $\mathbf{e}'_1$ is parallel to the generator of the cylindrical geometry.

Now points on the reference surface of the shell may be located by the position vector $\mathbf{R}$ given by

$$\mathbf{R} = x\mathbf{e}'_1 + R\mathbf{e}'_3, \qquad \theta^1 = x, \qquad \theta^2 = \gamma, \qquad (4.2a, b, c)$$

where we have identified the coordinates θ^1 and θ^2 with x and γ, respectively. Using the definitions in [3] and in Section 2, the relevant geometrical properties of the cylindrical surface may be recorded as

$$A^{1/2} = R, \qquad A^{11} = 1, \qquad A^{12} = 0, \qquad A^{22} = 1/R^2, \qquad (4.3a, b, c, d)$$

$$B_2^2 = -1/R, \qquad \text{all other } B_\beta^\alpha = 0, \qquad \Gamma_{\alpha\beta}^\sigma = 0. \qquad (4.3e, f, g)$$

Substituting (4.3) into (2.17), we have

$$\rho_0 = \rho_0^* h, \qquad B^+ = A^{1/2}(1 + h/2R), \qquad B^- = A^{1/2}(1 - h/2R). \qquad (4.4a, b, c)$$

It follows that the thermal equations (2.20) become

$$\rho_0^* ch\dot{\theta} = \rho_0^* h\theta_0 \hat{s} - (1 + h/2R)q^+ + (1 - h/2R)q^- + Kh\nabla^2\theta, \qquad (4.5a)$$

$$\frac{\rho_0^* ch^2}{\pi^2}\dot{\phi} = \rho_0^* \theta_0 \hat{s}_1 - \frac{1}{2}\left(1 + \frac{h}{2R}\right)q^+ - \frac{1}{2}\left(1 - \frac{h}{2R}\right)q^- - K\phi + \frac{Kh^2}{12}\nabla^2\phi, \qquad (4.5b)$$

where the Laplacian operator $\nabla^2\theta$ for the cylindrical geometry is given by

$$\nabla^2\theta = \frac{\partial^2\theta}{\partial x^2} + \frac{1}{R^2}\frac{\partial^2\theta}{\partial\gamma^2}. \qquad (4.6)$$

Problem 1: Here we consider the problem for which the heat flux on the outer surface is constant, the inner surface is insulated, external entropy supply is neglected, and the shell

† Although this coordinate system is unconventional, it is chosen because it yields convenient relations between $\mathbf{A}_i$ and $\mathbf{e}'_i$.

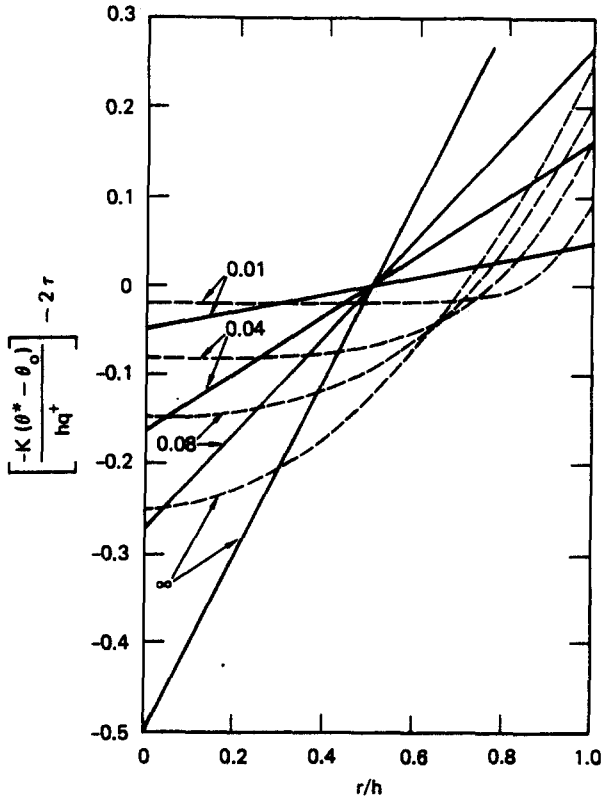

Fig. 7. Normalized temperature in a solid circular cylinder of radius h, with constant heat flux q^+ (out of the cylinder) at its surface and uniform initial temperature $\theta = \theta_0$. The numbers on the curved lines are values of $\tau = Kt/\rho_0^* ch^2$. The dashed lines are the exact solution, and the solid lines are the Cosserat solution.

is initially at uniform temperature θ_0. Hence the conditions (3.1) and (3.4) hold, and eqns (4.5) reduce to

$$\rho_0^* ch\dot{\theta} = -(1+h/2R)q^+, \tag{4.7a}$$

$$\rho_0^* ch\dot{\phi} = -K\phi - \tfrac{1}{2}(1+h/2R)q^+. \tag{4.7b}$$

Integrating (4.7) subject to the initial conditions (3.4c, d), we obtain

$$-K(\theta-\theta_0)/hq^+ = (1+h/2R)\tau, \tag{4.8a}$$

$$-K\phi/q^+ = \tfrac{1}{2}(1+h/2R)[1-\exp(-\pi^2\tau)], \tag{4.8b}$$

where τ is defined by (3.6). Notice that in the thin-shell limit ($R/h \to \infty$), the solution (4.8) approaches the plate solution (3.5). In the thick-shell limit of a solid cylinder for which† $R = h/2$, the right-hand side of (4.8a) becomes 2τ which is consistent with the exact solution[5 (p. 203)]. Using (2.16b), the Cosserat solution (4.8) with $R = h/2$, is plotted in Fig. 7 together with the exact solution for various values of the time parameter τ. The dashed lines in Fig. 7 have been taken directly from [5] (Fig. 25, p. 203), and r is the radial coordinate with $r = 0$ locating the center of the cylinder and $r = h$ locating the outer surface.

† From [3], we recall that generally $G^{1/2}$ is required to be positive. Although the quantity $G^{1/2}$ vanishes when $\theta^3 = -h/2$ and $R = h/2$, this poses no particular difficulty in the problems considered here.

In view of the form of solution (4.8), it is obvious that the long-time temperature is dominated by the term (4.8a). The fact that the coefficient of τ in (4.8a) yields the correct result even in the thick-shell limit suggests that the Cosserat theory retains the important geometrical features of the shell. In this regard, it is worth mentioning that the result (4.8a) could be obtained using an engineering approach in which the temperature in the shell is assumed to be uniform, and the energy entering the outer surface is equated with the increase in internal energy. It is also worth mentioning that the solution of the more accurate eqn (15) of [1] yields a long-time solution of the form

$$-\frac{K(\theta^*-\theta_0)}{hq^+} \to \left[\frac{\sinh(h/2R)+\cosh(h/2R)}{(2R/h)\sinh(h/2R)}\right]\tau. \tag{4.9}$$

In the thin-shell limit, (4.9) yields the correct result, but in the thick-shell limit, it yields the result (2.313τ), which is incorrect. Thus, even though eqn (15) of [1] is more complicated than eqns (4.8), it does not necessarily produce a better result.

Problem 2: To further examine the validity of the constitutive equations (2.14b, c) and the specifications (2.19a, c), we consider a simple problem for which the Laplacian operators in (4.5) do not vanish. Specifically, consider the steady-state problem of uniform heat conduction in the constant $\mathbf{e}_3$ direction for which the three-dimensional solution is given by

$$\mathbf{q}^* = Q\mathbf{e}_3, \qquad \theta^* = [\theta_0-(QR/K)\cos\gamma]-\theta^3[(Q/K)\cos\gamma], \tag{4.10a, b}$$

where $\mathbf{q}^*$ is the three-dimensional heat conduction vector, and Q is a constant. Using (4.1) and (4.10), we realize that

$$q^+ = q^- = \mathbf{q}^*\cdot\mathbf{e}_3' = Q\cos\gamma. \tag{4.11}$$

Consequently, in the absence of external entropy supply the steady-state solution of (4.5) becomes

$$\theta = \theta_0-(QR/K)\cos\gamma, \qquad \phi = -[1+(h^2/12R^2)]^{-1}(Q/K)\cos\gamma. \tag{4.12a, b}$$

Now, with the help of (2.16b), we may compare the exact result (4.10b) with the Cosserat result (4.12) to conclude that the average temperature is predicted exactly. Further, the prediction of the average temperature gradient ϕ is very accurate in the thin-shell limit ($R/h \to \infty$) and is only 25% low in the thick-shell limit ($R/h \to 1/2$).

5. SPHERICAL SHELLS

The spherical shell geometry is considered here mainly because it is one of the simplest geometries in which it is possible to investigate the differences between the constitutive assumptions (2.12) and (2.14). Three problems of a spherical shell of constant thickness h and radius R are considered. For the first two problems, we consider the thick-shell limit of a solid sphere and discuss the differences between assumptions (2.12) and (2.14). For the third problem, we consider the transition from a thick shell to a thin shell.

With reference to the Cartesian base vectors $\mathbf{e}_i$ introduced in Section 4, we let $\mathbf{e}_i''$ be base vectors of a spherical coordinate system with polar angle γ ($0 \leqslant \gamma \leqslant 2\pi$) measured from the $\mathbf{e}_1$–$\mathbf{e}_3$ plane and polar angle σ ($-\pi/2 \leqslant \sigma \leqslant \pi/2$) measured from the $\mathbf{e}_1$–$\mathbf{e}_2$ plane such that†

$$\mathbf{e}_1'' = -\sin\gamma\mathbf{e}_1+\cos\gamma\mathbf{e}_2, \tag{5.1a}$$

† Although this coordinate system is unconventional, it is chosen because it yields convenient relations between $\mathbf{A}_i$ and $\mathbf{e}_i''$.

$$\mathbf{e}_2'' = -\sin\sigma(\cos\gamma\mathbf{e}_1 + \sin\gamma\mathbf{e}_2) + \cos\sigma\mathbf{e}_3, \tag{5.1b}$$

$$\mathbf{e}_3'' = \cos\sigma(\cos\gamma\mathbf{e}_1 + \sin\gamma\mathbf{e}_2) + \sin\sigma\mathbf{e}_3. \tag{5.1c}$$

Now points on the reference surface of the shell may be located by the position vector $\mathbf{R}$ given by

$$\mathbf{R} = R\mathbf{e}_3'', \qquad \theta^1 = \gamma, \qquad \theta^2 = \sigma, \tag{5.2a, b, c}$$

where we have identified the coordinates θ^1 and θ^2 with γ and σ, respectively. Using the definitions in [3] and in Section 2, the relevant geometrical properties of the spherical surface may be recorded as

$$A^{1/2} = R^2\cos\sigma, \qquad A^{11} = 1/R^2\cos^2\sigma, \qquad A^{12} = 0, \qquad A^{22} = 1/R^2, \tag{5.3a, b, c, d}$$

$$B_1^1 = B_2^2 = -1/R, \qquad \text{all other } B_\beta^\alpha = 0, \tag{5.3e, f}$$

$$\Gamma_{12}^1 = \Gamma_{21}^1 = -\tan\sigma, \qquad \Gamma_{11}^2 = \sin\sigma\cos\sigma, \qquad \text{all other } \Gamma_{\alpha\beta}^\sigma = 0. \tag{5.3g, h, i}$$

Substituting (5.3) into (2.17), we have

$$\rho_0 = \rho_0^* h(1+h^2/12R^2), \quad B^+ = A^{1/2}(1+h/2R)^2, \quad B^- = A^{1/2}(1-h/2R)^2. \tag{5.4a, b, c}$$

It follows that the thermal equations (2.20) become

$$\rho_0^* ch\left(1+\frac{h^2}{12R^2}\right)\dot\theta = \rho_0\theta_0\hat s - \left(1+\frac{h}{2R}\right)^2 q^+ + \left(1-\frac{h}{2R}\right)^2 q^- + Kh\nabla^2\theta, \tag{5.5a}$$

$$\frac{\rho_0^* ch^3}{\pi^2}\left(1+\frac{h^2}{12R^2}\right)\dot\phi = \rho_0\theta_0\hat s_1 - \left(\frac{h}{2}\right)\left(1+\frac{h}{2R}\right)^2 q^+ - \left(\frac{h}{2}\right)\left(1-\frac{h}{2R}\right)^2 q^- - Kh\left(1+\frac{h^2}{12R^2}\right)\phi + \frac{Kh^3}{12}\nabla^2\phi, \tag{5.5b}$$

where the Laplacian operator $\nabla^2\theta$ for the spherical geometry is given by

$$\nabla^2\theta = \frac{1}{R^2\cos^2\sigma}\frac{\partial^2\theta}{\partial\gamma^2} + \frac{1}{R^2}\frac{\partial^2\theta}{\partial\sigma^2} - \frac{\tan\sigma}{R^2}\frac{\partial\theta}{\partial\sigma}. \tag{5.6}$$

Problem 1: For the first problem, the heat flux on the outer surface is constant, the inner surface is insulated, external entropy supply is neglected, and the shell is initially at uniform temperature θ_0. Hence the conditions (3.1) and (3.4) hold, and eqns (5.5) reduce to

$$\rho_0^* ch(1+h^2/12R^2)\dot\theta = -(1+h/2R)^2 q^+, \tag{5.7a}$$

$$\frac{\rho_0^* ch^2}{\pi^2}\left(1+\frac{h^2}{12R^2}\right)\dot\phi = -\frac{1}{2}\left(1+\frac{h}{2R}\right)^2 q^+ - K\left(1+\frac{h^2}{12R^2}\right)\phi. \tag{5.7b}$$

Integrating (5.7) subject to the initial conditions (3.4c, d), we obtain

$$-\frac{K(\theta-\theta_0)}{hq^+}=\frac{(1+h/2R)^2}{(1+h^2/12R^2)}\tau, \tag{5.8a}$$

$$-\frac{K\phi}{q^+}=\frac{(1+h/2R)^2}{2(1+h^2/12R^2)}[1-\exp(-\pi^2\tau)], \tag{5.8b}$$

where τ is defined by (3.6). Notice that in the thin-shell limit ($R/h \to \infty$), the solution (5.8) approaches the plate solution (3.5). In the thick-shell limit of a solid sphere for which $R = h/2$, the right-hand side of (5.8a) becomes 3τ which is consistent with the exact solution[5 (p. 242)]. Using (2.16b), the Cosserat solution (5.8) with $R = h/2$ is plotted in Fig. 8 together with the exact solution for various values of the time parameter τ. The dashed lines in Fig. 8 have been taken directly from [5] (Fig. 31, p. 242), and r is the radial coordinate with $r = 0$ locating the center of the sphere and $r = h$ locating the outer surface.

From Fig. 8, we observe that for long time the value of the average temperature gradient predicted by the Cosserat theory is substantially larger than the exact value. However, this is not particularly important because for long time the temperature is dominated by the term (5.8a). To exhibit this, we have used (2.17i, j) together with (5.8) to

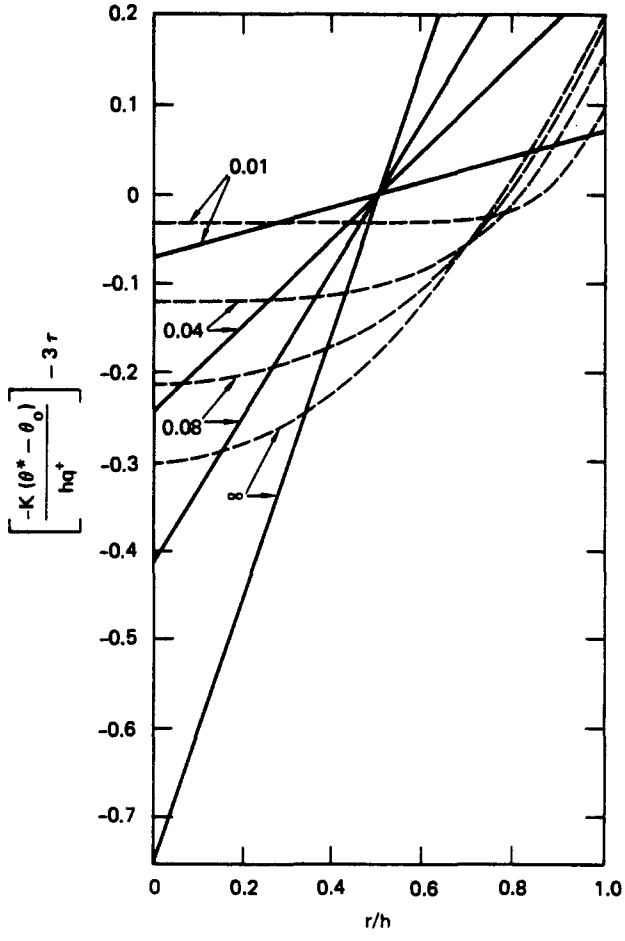

Fig. 8. Normalized temperature in a solid sphere of radius h, with constant heat flux q^+ (out of the sphere) at its surface and uniform initial temperature $\theta = \theta_0$. The numbers on the curves are values of $\tau = Kt/\rho_0^0 ch^2$. The dashed lines are the exact solution, and the solid lines are the Cosserat solution.

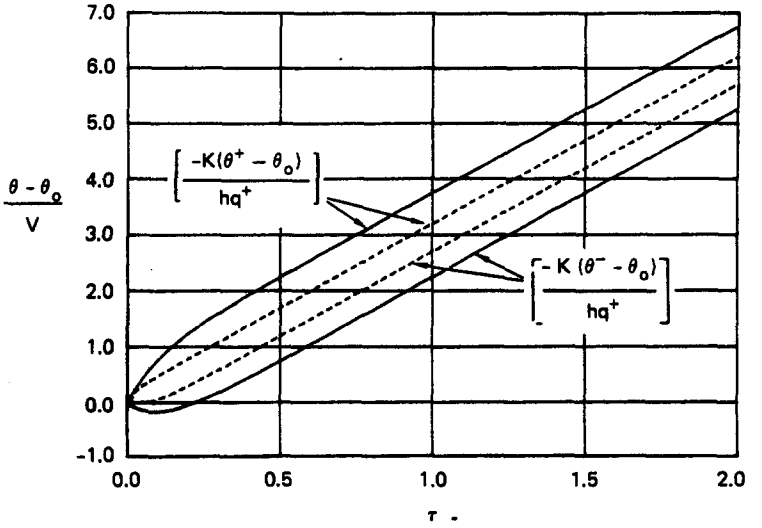

Fig. 9. Normalized temperature $[-K(\theta^+ - \theta_0)/hq^+]$ at the surface and $[-K(\theta^- - \theta_0)/hq^+]$ at the center of a solid sphere of radius h, with constant heat flux q^+ (out of the sphere) at its surface and uniform initial temperature $\theta = \theta_0$. The dashed lines are the exact solution, and the solid lines are the Cosserat solution. $\tau = Kt/\rho_0^* ch^2$.

plot in Fig. 9 the temperature on the outer surface and at the center of the solid sphere. The dashed lines in Fig. 9 represent the exact solution[5 (p. 242)]. For short time, the Cosserat theory predicts the incorrect result that the center temperature of the sphere drops. This is a consequence of the overprediction of the average temperature gradient. For long time, the lines in Fig. 9 are parallel, and the relative error diminishes to zero. This is because the prediction (5.8a) is exact in the thick-shell limit. In this regard, it is worth mentioning that the result (5.8a) could be obtained using the engineering approach described in Section 4. It is also worth mentioning that the more accurate eqn (15) of [1] yields a long-time solution of the form†

$$-\frac{K(\theta^* - \theta_0)}{hq^+} \to \left[\frac{\sinh(h/R) + \cosh(h/R)}{(R/h)\sinh(h/R)}\right]\tau. \tag{5.9}$$

In the thin-shell limit, (5.9) yields the correct result, but in the thick-shell limit, it yields the result (4.075τ), which is incorrect.

We are now in a position to comment on the differences between the constitutive eqns (2.12) and (2.14). If (2.12a) was used instead of (2.14a), then the average temperature would be given by

$$-K(\theta - \theta_0)/hq^+ = (1 + h/2R)^2\tau \tag{5.10}$$

instead of (5.8a). This would yield the incorrect result 4τ in the thick-shell limit. Similarly, if (2.12d, e) were used instead of (2.14d, e), then the long-time value of ϕ would be

$$-K\phi/q^+ = \tfrac{1}{2}(1 + h/2R)^2, \tag{5.11}$$

which produces a larger error than that associated with (5.8b) in the thick-shell limit.

Problem 2: To further examine the validity of constitutive equations (2.14b, c) and the specifications (2.19a, c), we consider the steady-state problem of uniform heat conduction

† The solution in Appendix A of [1] should be written in a form which has a linear term in time.

in the constant $\mathbf{e}_1$ direction for which the three-dimensional solution is given by

$$\mathbf{q}^* = Q\mathbf{e}_1, \qquad \theta^* = [\theta_0 - (QR/K)\cos\gamma\cos\sigma] - \theta^3[(Q/K)\cos\gamma\cos\sigma], \quad (5.12a, b)$$

where $\mathbf{q}^*$ is the three-dimensional heat conduction vector, and Q is a constant. Using (5.1) and (5.12), we realize that

$$q^+ = q^- = \mathbf{q}^* \cdot \mathbf{e}_3'' = Q\cos\gamma\cos\sigma. \quad (5.13)$$

Consequently, in the absence of external entropy supply, the steady-state solution of (5.5) becomes

$$\theta = \theta_0 - (QR/K)\cos\gamma\cos\sigma, \qquad \phi = -(Q/K)\cos\gamma\cos\sigma, \quad (5.14a, b)$$

which is an exact result valid for both the thin- and thick-shell limits.

Problem 3: Finally, to examine the transition from a thin-shell to a thick-shell, we consider the steady-state problem where the temperature θ^+ on the outer surface is specified to be the constant value θ_0, and the heat flux q^- on the inner surface is constant. Thus, using (2.17i), we require

$$\theta + (h/2)\phi = \theta_0, \qquad q^- = \text{const.} \quad (5.15a, b)$$

In the absence of external entropy supply, the steady-state solution of (5.5) becomes

$$\frac{K(\theta - \theta_0)}{hq^-} = \frac{(1 - h/2R)^2}{2(1 + h^2/12R^2)}, \qquad \frac{K\phi}{q^-} = -\frac{(1 - h/2R)^2}{(1 + h^2/12R^2)}, \quad (5.16a, b)$$

$$\frac{q^+}{q^-} = \frac{(1 - h/2R)^2}{(1 + h/2R)^2}. \quad (5.16c)$$

It can be shown that the exact solution[5 (p. 247)] may be written in the form

$$\frac{K(\theta^* - \theta_0)}{hq^-} = \frac{(1 - h/2R)^2(1 - 2\theta^3/h)}{2(1 + h/2R)(1 + \theta^3/R)}, \quad (5.17)$$

and that (5.16c) is an exact result. Now to compare the predictions (5.16) with the exact solution (5.17), we have used (2.16b) to plot (5.16) as the solid lines in Fig. 10 and have used (5.17) to plot the dashed lines in Fig. 10 for three values of R/h. The results in Fig. 10 show again that the Cosserat predictions are good even for a fairly thick shell ($R/h = 1$).

6. CONICAL SHELL

In the previous sections, we have solved a number of problems for plates, circular cylindrical shells and spherical shells to develop confidence that the Cosserat theory can predict relatively accurate results for both the thin-shell limit (which models the base of a conical shell) and the thick-shell limit (which models the tip of a conical shell). Here we confine attention to a conical shell with constant thickness h and locate points on the conical surface by

$$\mathbf{R} = \beta R\mathbf{e}_1' + R\mathbf{e}_3', \qquad \theta^1 = R, \qquad \theta^2 = \gamma, \quad (6.1a, b, c)$$

where R is the radial coordinate, γ is the polar angle, $\mathbf{e}_i'$ are defined by (4.1), β is a constant related to the cone angle (see Fig. 1), and we have identified the coordinates θ^1 and θ^2 with R and γ, respectively. Using the definitions in [3] and in Section 2, the relevant

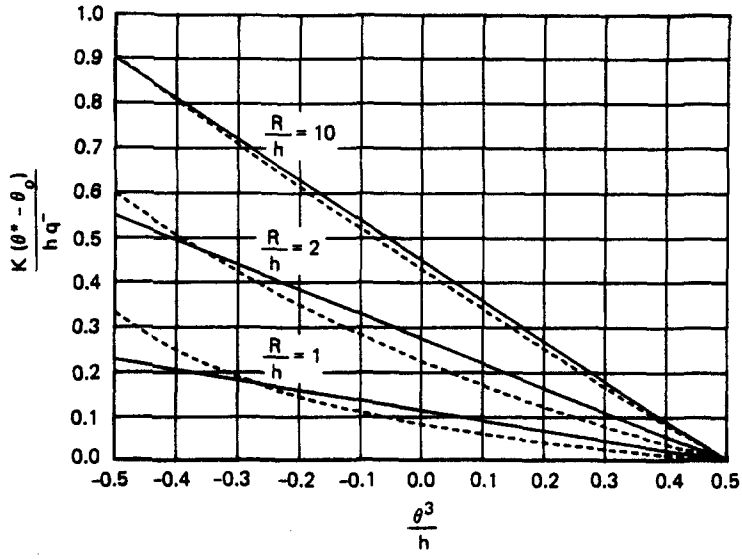

Fig. 10. The normalized steady state temperature in a spherical shell with constant thickness h and mean radius R. The heat flux q^- (entering the shell) is specified on the inner surface and the temperature $\theta^+ = \theta_0$ is specified on the outer surface. The dashed lines are the exact solution, and the solid lines are the Cosserat solution.

geometrical properties of the conical surface may be recorded as

$$A^{1/2} = R(1+\beta^2)^{1/2}, \qquad A^{11} = 1/(1+\beta^2), \qquad A^{12} = 0, \qquad A^{22} = 1/R^2, \tag{6.2a, b, c, d}$$

$$B_2^2 = -\beta/R(1+\beta^2)^{1/2}, \qquad \text{all other } B_\beta^\alpha = 0, \tag{6.2e, f}$$

$$\Gamma_{22}^1 = -R/(1+\beta^2), \qquad \Gamma_{12}^2 = \Gamma_{21}^2 = 1/R, \qquad \text{all other } \Gamma_{\alpha\beta}^\sigma = 0. \tag{6.2g, h}$$

Substituting (6.2) into (2.17), we have

$$\rho_0 = \rho_0^* h, \qquad B^+ = A^{1/2}\left[1 + \frac{h\beta}{2R(1+\beta^2)^{1/2}}\right], \qquad B^- = A^{1/2}\left[1 - \frac{h\beta}{2R(1+\beta^2)^{1/2}}\right]. \tag{6.3a, b, c}$$

It follows that the thermal equations (2.20) become

$$\rho_0^* ch\dot{\theta} = \rho_0^* h\theta_0 \hat{s} - \left[1 + \frac{h\beta}{2R(1+\beta^2)^{1/2}}\right]q^+ + \left[1 - \frac{h\beta}{2R(1+\beta^2)^{1/2}}\right]q^- + Kh\nabla^2\theta, \tag{6.4a}$$

$$\frac{\rho_0^* ch^2}{\pi^2}\dot{\phi} = \rho_0^* \theta_0 \hat{s}_1 - \frac{1}{2}\left[1 + \frac{h\beta}{2R(1+\beta^2)^{1/2}}\right]q^+ - \frac{1}{2}\left[1 - \frac{h\beta}{2R(1+\beta^2)^{1/2}}\right]q^- - K\phi + \frac{Kh^2}{12}\nabla^2\phi, \tag{6.4b}$$

where the Laplacian operator $\nabla^2\theta$ for the conical geometry is given by

$$\nabla^2\theta = \frac{1}{(1+\beta^2)}\left[\frac{1}{R}\frac{\partial}{\partial R}\left(R\frac{\partial\theta}{\partial R}\right) + \frac{(1+\beta^2)}{R^2}\frac{\partial^2\theta}{\partial\gamma^2}\right]. \tag{6.5}$$

Here we consider the problem for which the heat flux on the outer surface is constant, all other surfaces are insulated, external entropy supply is neglected, and the shell is initially at uniform temperature θ_0. Hence the conditions (3.4) hold in addition to the conditions

$$\theta = \theta(R, t), \qquad \phi = \phi(R, t), \tag{6.6a, b}$$

$$\partial\theta/\partial R = 0, \qquad \partial\phi/\partial R = 0, \qquad \text{at } R = R_1, R_2 \tag{6.6c, d}$$

where R_1 and R_2 are the tip radius and base radius of the shell, respectively (see Fig. 1). Under these conditions, eqns (6.4) reduce to

$$\rho_0^* ch\dot{\theta} = -\left[1 + \frac{h\beta}{2R(1+\beta^2)^{1/2}}\right]q^+ + \frac{Kh}{R(1+\beta^2)}\frac{\partial}{\partial R}\left(R\frac{\partial\theta}{\partial R}\right), \tag{6.7a}$$

$$\frac{\rho_0^* ch^2}{\pi^2}\dot{\phi} = -\frac{1}{2}\left[1 + \frac{h\beta}{2R(1+\beta^2)^{1/2}}\right]q^+ - K\phi + \frac{Kh^2}{12R(1+\beta^2)}\frac{\partial}{\partial R}\left(R\frac{\partial\phi}{\partial R}\right). \tag{6.7b}$$

To analyze these equations, it is convenient to introduce the nondimensional parameters

$$z = R/h, \qquad \tau = Kt/\rho_0^* ch^2, \tag{6.8a, b}$$

$$\bar{\theta} = \bar{\theta}(z, \tau) = -K(\theta - \theta_0)/hq^+, \qquad \bar{\phi} = \bar{\phi}(z, \tau) = -K\phi/q^+, \tag{6.8c, d}$$

and rewrite them in the form

$$\frac{\partial\bar{\theta}}{\partial\tau} - \frac{1}{(1+\beta^2)}\frac{1}{z}\frac{\partial}{\partial z}\left(z\frac{\Delta\bar{\theta}}{\partial z}\right) = \left[1 + \frac{\beta}{2z(1+\beta^2)^{1/2}}\right], \tag{6.9a}$$

$$\frac{\partial\bar{\phi}}{\partial\tau} + \pi^2\bar{\phi} - \frac{\pi^2}{12(1+\beta^2)}\frac{1}{z}\frac{\partial}{\partial z}\left(z\frac{\partial\bar{\phi}}{\partial z}\right) = \frac{\pi^2}{2}\left[1 + \frac{\beta}{2z(1+\beta^2)^{1/2}}\right]. \tag{6.9b}$$

Similarly, the initial conditions (3.4c, d) and boundary conditions (6.6c, d) become

$$\bar{\theta} = 0, \qquad \bar{\phi} = 0, \qquad \text{at } \tau = 0, \tag{6.10a, b}$$

$$\partial\bar{\theta}/\partial z = 0, \qquad \partial\bar{\phi}/\partial z = 0, \qquad \text{at } z = z_1, z_2, \tag{6.10c, d}$$

where z_1 and z_2 are the values of z when R equals R_1 and R_2, respectively. At this point, it is of interest to note that in the limit of large β ($\beta \to \infty$), eqns (6.9) reduce to a nondimensional form of (4.7) for a circular cylindrical shell, and in the limit of small β ($\beta \to 0$), eqns (6.9) characterize a circular plate.

Using standard techniques, the solution of (6.9) may be written in the form

$$\bar{\theta} = A_0(\tau) + \sum_{m=1}^{\infty} A_m(\tau) f_m(z), \tag{6.11a}$$

$$\bar{\phi} = B_0(\tau) + \sum_{m=1}^{\infty} B_m(\tau) f_m(z). \tag{6.11b}$$

where $f_m(z)$ are eigenfunctions characterized by

$$\frac{1}{z}\frac{\mathrm{d}}{\mathrm{d}z}\left(z\frac{\mathrm{d}f_m}{\mathrm{d}z}\right) = -\alpha_m^2 f_m \qquad \text{(no sum on } m) \tag{6.12a}$$

$$\mathrm{d}f_m/\mathrm{d}z = 0, \qquad \text{at } z = z_1, z_2, \tag{6.12b}$$

and where α_n^2 are the nonzero eigenvalues. Since eqn (6.12a) can easily be recognized as Bessel's equation of order zero, the solution, subject to the boundary conditions (6.12b), is well characterized and may be written in the form

$$f_m(z) = J_0(\alpha_m z) - \frac{J_1(\alpha_m z_1)}{Y_1(\alpha_m z_1)} Y_0(\alpha_m z), \tag{6.13}$$

where J_n and Y_n are Bessel functions of the first and second kind, respectively, of order n, and where α_m are the positive roots of the characteristic equation

$$J_1(\alpha_m z_1) Y_1(\alpha_m z_2) - Y_1(\alpha_m z_1) J_1(\alpha_m z_2) = 0. \tag{6.14}$$

Further, the eigenfunctions f_m satisfy the orthogonality conditions

$$\int_{z_1}^{z_2} z f_m \, dz = 0, \qquad \int_{z_1}^{z_2} z f_m f_n \, dz = 0, \qquad \text{for } (m \neq n). \tag{6.15a, b}$$

Substituting (6.11) into (6.9), multiplying the result by z and integrating, multiplying the result by zf_n and integrating, and using the orthogonality conditions (6.15) and the initial conditions (6.10a, b), we conclude that

$$A_0(\tau) = C_0 \tau, \qquad C_0 = \left[1 + \frac{\beta}{(1+\beta^2)^{1/2}} \left(\frac{1}{z_1 + z_2}\right)\right]. \tag{6.16a, b}$$

$$A_m(\tau) = \frac{(1+\beta^2) C_m}{\alpha_m^2} \left[1 - \exp\left\{-\left(\frac{\alpha_m^2}{1+\beta^2}\right)\tau\right\}\right], \tag{6.16c}$$

$$C_m = \frac{(\beta/2(1+\beta^2)^{1/2}) \int_{z_1}^{z_2} f_m \, dz}{\int_{z_1}^{z_2} z f_m^2 \, dz}, \tag{6.16d}$$

$$B_0(\tau) = \tfrac{1}{2} C_0 [1 - \exp(-\pi^2 \tau)], \tag{6.16e}$$

$$B_m(\tau) = \frac{6 C_m}{12 + \alpha_m^2/(1+\beta^2)} \left[1 - \exp\left\{-\frac{\pi^2}{12}\left(12 + \frac{\alpha_m^2}{1+\beta^2}\right)\tau\right\}\right]. \tag{6.16f}$$

For later reference, we observe that if the dependence on z is neglected in (6.11), then (6.11) has the same form as the solution (4.8). This means that we would be essentially modeling the conical shell as an "equivalent" circular cylindrical shell with "mean" radius $R/h = (z_1 + z_2)(1+\beta^2)^{1/2}/2\beta$. By considering a specific example, it will be shown that making this kind of engineering approximation introduces significant errors at the tip of the conical shell.

Consider the specific example of the conical shell drawn in Fig. 1 which has a solid tip. For this shell we specify

$$z_1 = \beta/2(1+\beta^2)^{1/2}, \qquad z_2 = 15, \qquad \beta = 3.23. \tag{6.17a, b, c}$$

The minimum value z_1 of z given by (6.17a) is specified by requiring the inner surface of the shell to just make contact at the shell's tip. Using (6.17), we have solved for the first 20 eigenvalues and eigenfunctions and have plotted the solution (6.11) in Figs. 11 and 12 by normalizing the results by the first terms in the solutions. Figure 11 shows plots of $\bar{\theta}/A_0(\tau)$ vs z for various values of τ, and Fig. 12 shows plots of $\bar{\phi}/B_0(\tau)$ vs z for two values

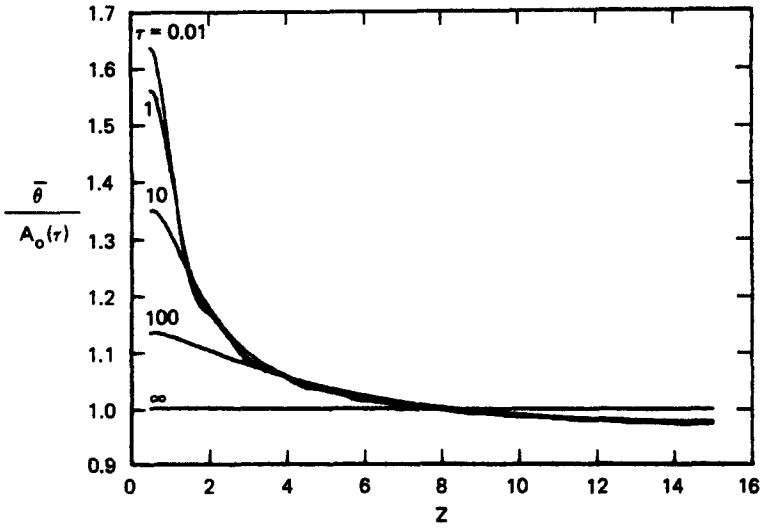

Fig. 11. Normalized average temperature in a conical shell of thickness h. The numbers on the curves are values of $\tau = Kt/\rho_0^* ch^2$.

of τ. The slight waviness in these curves is caused by the fact that we have approximated solutions (6.11a, b) using finite series.

From Fig. 11, we observe that for long time the average temperature is relatively uniform over the shell. This is because the equivalent-cylinder solution $A_0(\tau)$ dominates for long time. However, for short time the value of $\bar{\theta}$ at the tip is about 65% greater than that predicted by the equivalent-cylinder solution. This result can be explained by observing from (4.8a) that a thick cylinder heats up faster than a thin cylinder. Thus we would expect the tip of the conical shell, which is thick, to heat up faster than its base, which is thin. From Fig. 12, we observe that the distribution of the average temperature gradient is nearly constant with time. Also, the value of $\bar{\phi}$ near the tip is nearly 65% greater than the value predicted by the equivalent-cylinder solution.

To exhibit the temporal dependence of this solution more clearly, we have plotted $A_0(\tau)$ and $B_0(\tau)$ in Fig. 13. From this figure, we observe that $B_0(\tau)$ reaches its maximum value in a relatively short time. Recalling [3], that the average temperature gradient is

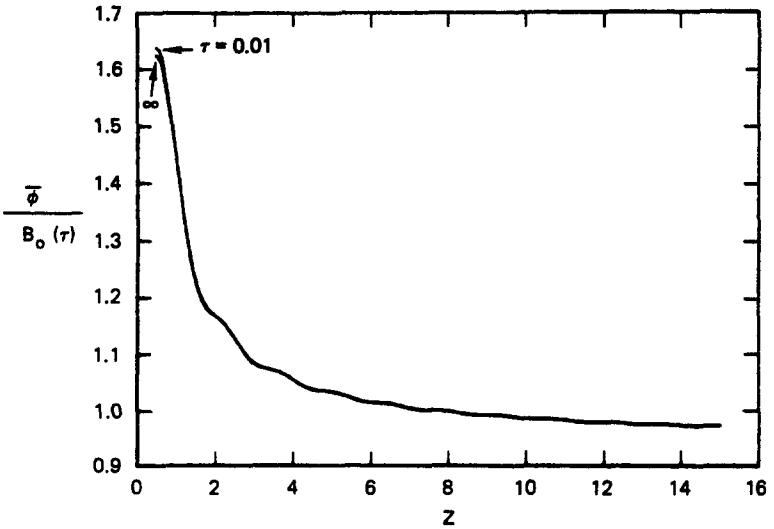

Fig. 12. Normalized average temperature gradient in a conical shell of thickness h. The numbers on the curves are values of $\tau = Kt/\rho_0^* ch^2$.

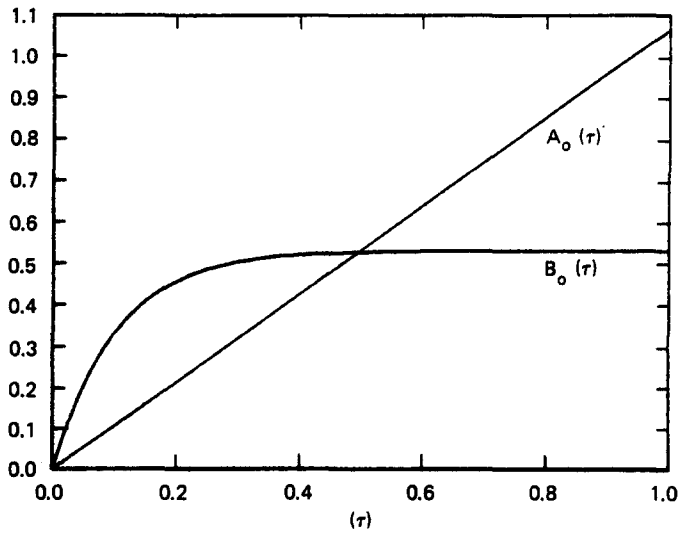

Fig. 13. Values of the functions $A_0(\tau)$ and $B_0(\tau)$ associated with the conical shell solution.

related to the thermal bending moment in the shell, this means that the bending in a conical shell under this load will be quite severe at its tip, and the full effect of the load will be felt in a relatively short time. Consequently, the tip of the conical shell should be particularly vulnerable to this type of thermal load.

7. SUMMARY

In this paper, we have focused attention on analyzing heat conduction in a rigid conical shell (Fig. 1). The conical shell is particularly interesting because it has a converging geometry, so that the shell near its tip is necessarily "thick" even though the shell near its base may be "thin". Further, the heat conduction equation is not separable for the conical geometry, so that it is exceedingly difficult to obtain exact solutions. Here we have chosen to model the shell with the theory of a Cosserat surface to determine the average (through-the-thickness) temperature and temperature gradient in the shell directly, without resorting to integration of three-dimensional results.

A number of problems of plates, circular cylindrical shells and spherical shells are considered, and the solutions are compared with exact solutions to develop confidence in the Cosserat theory. Within the context of this theory, it is usually assumed that constitutive equations for shells have the same form as those for plates. Here it is shown that in order to predict relatively accurate results in the thick-shell limit, it is necessary to generalize these constitutive equations to include certain geometrical features of the shell. The generalized constitutive equations are developed here in a consistent manner and tested in the thick-shell limit. The tests include problems where the temperature fields θ and ϕ are functions of time only, so that their Laplacian vanishes, as well as problems where they are functions of space only, and their Laplacian does not vanish. In all cases, satisfactory results are predicted even in the thick-shell limit.

Finally, a problem of transient heat conduction in a conical shell, which does not have an exact solution, is solved analytically using the Cosserat theory. It is shown that both the average temperature and temperature gradient have values near the tip which are about 65% greater than those predicted by an approximate equivalent-cylinder solution. Also, it is shown that the thermal bending moment produced by the average temperature gradient is quite severe near the tip, and it attains its maximum value in a relatively short time.

Acknowledgement—This research was supported by the U.S. Air Force Office of Scientific Research under Contract F49620-84K-0001 with SRI International, Menlo Park, California. The author would also like to acknowledge Mrs B. Bain for her help with the numerical calculations in this paper.

REFERENCES

1. M. A. Brull and J. R. Vinson, Approximate three-dimensional solutions for transient temperature distribution in shells of revolution. *J. Aero. Sci.* **25**, 742–750 (1958).
2. P. M. Naghdi, On the non-linear thermoelastic theory of shells. In *Non-Classical Shell Problems*, Proc. I.A.S.S. Symp., pp. 5–26. North-Holland, New York (1964).
3. A. E. Green and P. M. Naghdi, On thermal effects in the theory of shells. *Proc. R. Soc. London* **A365**, 161–190 (1979); **A367**, 572 (1979).
4. P. M. Naghdi, The theory of shells and plates. In *S. Flügge's Handbuch der Physik* (Edited by C. Truesdell), Vol. VIa/2, pp. 425–640. Springer-Verlag, Berlin (1972).
5. H. S. Carslaw and J. C. Jaeger, *Conduction of Heat in Solids*. Oxford Univ. Press, New York (1973).
6. M. B. Rubin, On the determination of certain constitutive coefficients for thermoelastic shells, to be published.